Nanoscale

COMMUNICATION

View Article Online
View Journal | View Issue

Cite this: *Nanoscale*, 2015, **7**, 10344

Received 28th March 2015,
Accepted 11th May 2015

DOI: 10.1039/c5nr01999k

www.rsc.org/nanoscale

Symmetry breaking polymerization: one-pot synthesis of plasmonic hybrid Janus nanoparticles†

Yanming Wang,[a] Tao Ding,*[a,b] Jeremy J. Baumberg[b] and Stoyan K. Smoukov*[a]

Asymmetric hybrid nanoparticles have many important applications in catalysis, nanomotion, sensing, and diagnosis, however ways to generate the asymmetric hybrid nanoparticles are quite limited and inefficient. Most current methods rely on interfacial adhesion and modification of already formed particles. In this article we report a one-pot, facile and scalable synthesis of anisotropic Au-polymer hybrid nanoparticles *via* interfacial oxidative dispersion polymerization. The interfacial nucleation and polymerization lead to spontaneous symmetry breaking and formation of the Janus particles. The reaction is initiated by monomer radicals generated by the strong oxidant $HAuCl_4$, which is itself later reduced by the electron-rich monomers to self-nucleate and form Au nanoparticles (NPs). The competition between divinylbenzene adsorption and the PVP capping agent results in effective partial surface wetting, forming asymmetric Au-PDVB hybrid nanoparticles, by confining growth of each material to its own phase. Such spontaneous symmetry breaking, important in morphogenesis, with control over the subsequent growth processes should lead to significant advances in the synthesis of asymmetric nanostructures.

1. Introduction

Asymmetric hybrid nanoparticles and their self-assemblies have become intriguing for a wide range of applications in optics[1–5] catalysis,[6] sensing,[7] and are key to creating increasingly complex nano-architectures.[8] Au-polymer composites are of special importance for theranostics because the metallic cores can function as a SERS substrate for sensitive biomolecular detection and the polymer shells can be used as carriers for drug delivery. The asymmetric configuration adds additional control upon aggregation for generating hot spots from contacts, which can be applied for photothermal therapy.[9]

Methods to generate Janus hybrid nanoparticles, however, are quite limited and always involve multi-steps, often relying on interfacial adhesion and partial modification of one part of a particle. One approach is self-assembly of di-block copolymers on the surface of Au NPs *via* hydrophobic interactions, however the thickness of such polymer shells is not tuneable.[10] The other route is dispersion polymerization of PS in the presence of Au seeds. Because of the incompatible surface potential between Au and PS, anisotropic growth was observed but required sophisticated control of the addition time of the Au seeds.[11] More recently, we have developed anisotropic hybrid nanoparticles based on the nonlinear swelling properties of highly cross-linked polymers, where the sizes of both Au and the polymer components are tuneable with good reproducibility.[12] That method, however, yields Au nanoparticles fully encapsulated inside the polymer matrix, which blocks the easy access of molecules to the gold surface for SERS measurements. Moreover, all of these methods need multiple steps which involve synthesis of the seeds and subsequent coating of the polymers, using different temperatures, solvents, and reagents. Therefore, reducing the number of reaction steps greatly improves the sustainability of these reactions, and a one-pot synthesis of these anisotropic hybrid nanoparticles is highly desirable for easy, scalable and cost-effective production.

Several groups have attempted one-pot syntheses of the asymmetric Au-polymer hybrid nanoparticles either *via* electrostatic repulsion,[13] or *in situ* reduction in phase-separated block polymers,[14] or with the assistance of liquid–liquid interfaces.[15] The mechanism of generating the asymmetric nanoparticles mostly relies on the balance of the interfacial tensions between the solid nanoparticles, soft polymers, and liquid solvent.[16–18]

In this communication, we demonstrate one-pot bulk synthesis of Janus nanoparticles made of Au and poly(divinylbenzene)

[a]*Department of Materials Science and Metallurgy, 27 Charles Babbage Road, University of Cambridge, CB3 0FS, UK. E-mail: dt413@cam.ac.uk, sks46@cam.ac.uk; Tel: +44 (0) 1223 334435*

[b]*Nanophotonics Centre, Cavendish Laboratory, University of Cambridge, CB3 0HE, UK*

†Electronic supplementary information (ESI) available: TEM images of hybrid nanoparticles formed wihout PVP, and hybrid nanoparticles formed at room temperature. See DOI: 10.1039/c5nr01999k

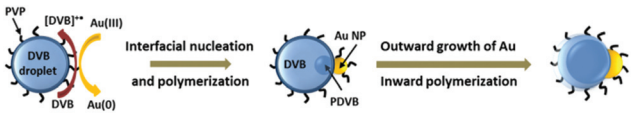

Scheme 1 Formation mechanism of Au-PDVB hybrid Janus colloidal particles.

(PDVB). We started from modified dispersion polymerization where $HAuCl_4$ was used as the initiator. The monomer droplets made of DVB were stabilised by polyvinylpyrrolidone (PVP) and oxidized by the $HAuCl_4$ to form a radical species which incurred further polymerization inside the droplets, while the $HAuCl_4$ was reduced to Au (0) to form Au NPs at the surface of the droplets (Scheme 1). There is an unfavourable interfacial energy mismatch between Au NPs (8.78 N m^{-1} with respect to vacuum, hydrophilic) and DVB (40 mN m^{-1}, hydrophobic),[19] which can initially lead to only partial capping of the Au NP nuclei by PDVB. Practically however, small levels of contaminants greatly influence the Au surface energy. To eliminate variations, we have used an excess of PVP capping agent which reproducibly controls the Au surface energy. In our case, the PVP also acts as a steric stabilizer for the DVB droplets. The DVB (or styrene), then competes with PDVB for adsorption and access to the surface to form the polymer part of the particles. This is different from our previous report where Au seeds facilitated initial uniform polymer coating around the Au NPs made asymmetric *via* a polymer swelling instability.[12] Instead, the interface between water and DVB droplet provides favourable nucleation sites for Au nuclei to form, followed by anisotropic growth: the metallic part grows much faster in the opposite direction of the part capped with polymers because of the self-catalytic process.[7] Further reduction and oxidative polymerization leads to independent growth kinetics of Au and PDVB components, which eventually leads to the formation of anisotropic hybrid nanoparticles (Scheme 1).

2. Experimental

2.1 Materials

Trihydrate gold tetrachloride ($HAuCl_4{\cdot}3H_2O$, 99%), Styrene (St, 90%), Divinyl benzene (DVB, 20% isomers) and Polyvinylpyrrolidone (PVP, M_w = 40 000) were purchased from Sigma-Aldrich company. All the water used in the experiments was deionised before use.

2.2 One-step synthesis of Au/PDVB asymmetric hybrid nanoparticles

An aqueous solution of PVP and $HAuCl_4$ was vortexed within a 1.5 ml eppendorf tube followed by the addition of DVB. The amount of $HAuCl_4$ and DVB could be adjusted and the resulting morphology of the hybrid nanoparticles changed accordingly. For the optimal synthesis of uniform Au/PDVB hybrid nanoparticles, 10 μl of $HAuCl_4$ (10 mM) and 40 μl of PVP (20 mg ml^{-1}) were added into 0.5 ml water. Another 1 μl of DVB (or diluted with 10 μl toluene) was injected after which strong ultrasonication (600 W) was applied to disperse the DVB in water to form a milky suspension. The Au reduction and DVB polymerization happened spontaneously, and occurred while the system was kept constantly in an ultrasonic bath (45 °C) for 2 h. Centrifugation (2000 rpm) was applied to separate large aggregates and impurities from the hybrid nanoparticles in the batch. The final products were stored in pure water.

2.3 Characterizations

SEM images were captured on a LEO 1530VP (Zeiss) at an accelerating voltage of 5 kV and with EDX mapping at 15 kV. The TEM images were taken under 100 kV. The samples were stained with $(NH_4)_6Mo_7O_{24}$ for clear imaging of the polymer parts. Dynamic light scattering (DLS) was performed with a Zetasizer (Malvern) to determine the size of the particles. Extinction spectra were measured with fiber coupled spectrometer (USB 2000, Ocean Optics).

3. Results and discussion

The synthesis of the asymmetric hybrid nanoparticles is based on dispersion polymerization, with spontaneous symmetry breaking, which allows the growth of two separate phases in different directions. Here $HAuCl_4$ is the strong oxidant for the generation of radical species of DVB, which initiates the well-established oxidative polymerization process, previously applied to the synthesis of polypyrrole and polyaniline.[17,20] In our case, the DVB has a divinyl functional group on the benzene ring, which is highly efficient in generating radicals for polymerization compared to styrene. The two vinyl bonds also introduce cross-linking in the polymer matrix. We use water as the dispersant and PVP as the stabilization agent.

The Au NPs are formed by interfacial nucleation, where the $HAuCl_4$ is reduced to Au(0) and self-nucleated to form Au NPs. Both the reduction and polymerization processes have very fast reaction kinetics and the formation of Au NPs and PDVB deposition happen simultaneously. Further reduction of Au(III) to Au(0) can also be self-catalyzed and selectively deposited on the surface of gold nanoparticles.[7] Here, PVP plays an important role in sterically stabilizing the small monomer droplets, on which Au NPs nucleate and grow. Without PVP these hybrid droplets coalesce, and thus only large droplets decorated with multiple Au NPs were formed (see ESI-Fig. S1†). At the initial stages of polymerization, the interfacial environment between DVB droplet and aqueous phases helps nucleate the Au NPs, but because of the large interfacial tension between the Au NPs, PDVB and H_2O, the PDVB and Au surfaces partially dewet[16] as they grow. In the end, the asymmetric hybrid nanoparticles of Au/PDVB are generated as shown in Fig. 1. The TEM and SEM images in Fig. 1a, b show the anisotropic encapsulation of the Au NPs and the EDX composition mapping further identifies the distribution of the PDVB and

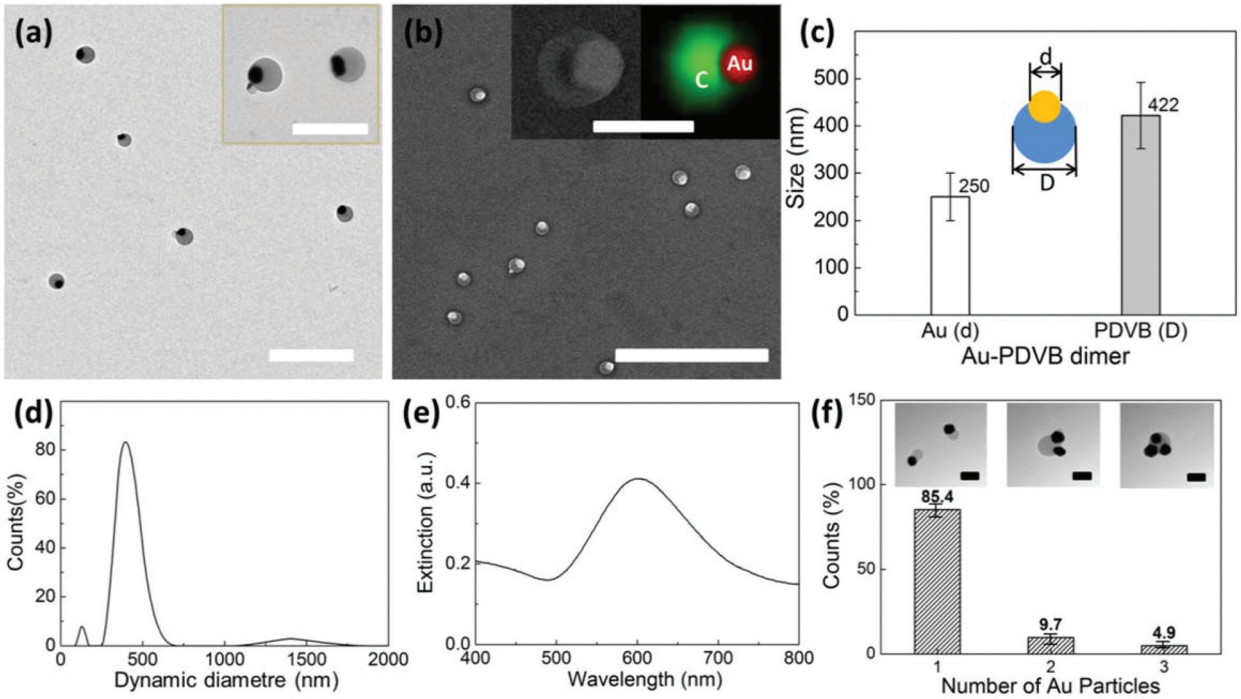

Fig. 1 Asymmetric hybrid nanoparticles synthesized with 0.2 mM $HAuCl_4$ and 32 mM DVB. (a) TEM image, scale bar is 2 μm and 1 μm in the inset, (b) SEM image with inset of EDX mapping. Scale bars are 5 μm and 500 nm in the inset, (c) is the statistic measurement of the sizes of the hybrid nanoparticles, (d) is the dynamic light scattering measurement of the hybrid nanoparticles in aqueous dispersion (number average), (e) is the UV-Vis spectra of the hybrid nanoparticles, (f) is the purity and the yield of the hybrid particles with different morphologies, all the scale bars in the insets are 100 nm.

Au NP components. The UV-Vis absorption (Fig. 1e) shows a distinctive plasmon absorption peak of the Au NPs at 600 nm. This wavelength results not only from the large size of the Au NPs but also from the change of refractive index from the polymer environment around them.[21] The asymmetric hybrid particles are relatively uniform upon purification. The diameter distribution was determined by comparison of two independent techniques, from the electron microscope images and statistical measurements of their sizes (Fig. 1c), and DLS (Fig. 1d). For example, the hybrid nanoparticles obtained under the condition for Fig. 1, had a component of Au with diameter of 250 nm and PDVB with size of 422 nm. The DLS hydrodynamic diameter was measured to be 450 nm for the hybrid nanoparticles (Fig. 1d), which is consistent with the size measured from TEM images. There were two minor impurities, sub-100 nm particles from later stage nucleation of Au NPs and >1 μm large polymer aggregates.

Around 15% of the PDVB hybrid nanoparticles in the batch, which was extracted after 20 min of polymerization, had two (<10%) or three (<5%) Au NPs on their surface (see Fig. 1f). Rather than multiple nucleation of Au particles, as observed under different conditions later, the same size of the Au particles on the surface indicate limited coalescence of the PDVB cores, even in the presence of PVP.

To maximize the yield of particles with only one PVDB and one AuNP core, it is critical to map out the effect of adjusting the concentration of the monomers and oxidant. Therefore, different concentrations of $HAuCl_4$ and DVB were utilised and the resulting reaction phase diagram is shown in Fig. 2. For high concentrations of $HAuCl_4$ (>1 mM) and DVB (>80 mM), faster reaction kinetics leads to multiple nucleation sites on a

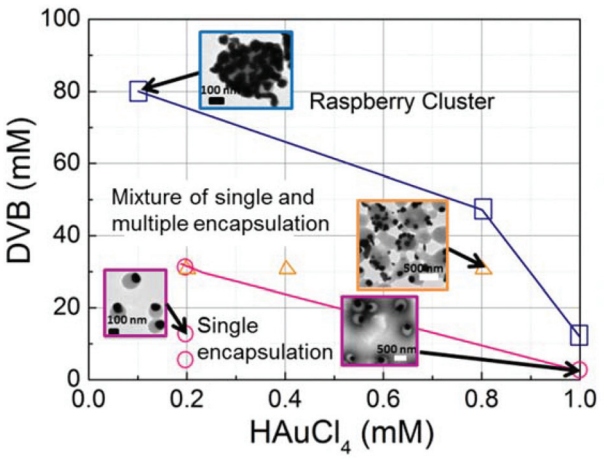

Fig. 2 The product diagram of hybrid nanoparticles under different concentrations of DVB and $HAuCl_4$. □ Au raspberry clusters, △ mixture of Au-PDVB nanoparticles with single and multiple Au components, ○ Au-PDVB Janus particles. The reactions are taking place under 45 °C.

single DVB droplet and coalescence of the droplets into raspberry-like clusters (the blue rectangles show reaction conditions tested). Intermediate concentrations of $HAuCl_4$ and DVB lead to the formation of anisotropic hybrid nanoparticles with a mixture of one and multiple Au nanoparticles on a single PDVB particle (indicated by orange triangles). Though these concentrations still favour high Au nucleation, the lower coalescence is the result of lowering the DVB/PVP ratio. Keeping the PVP concentration constant but lowering the DVB concentration makes it less competitive for binding to the surface and decreases the chance of coalescence between the particles at the initial stage of dispersion polymerization. When the concentration of DVB is lower than 16 mM and the concentration of $HAuCl_4$ was kept below 0.4 mM (purple circles), relative uniform Au-PDVB anisotropic particles were formed, with one AuNP per PDVB particle. Further lowering the concentration of DVB leads to Au-PDVB Janus nanoparticles which are smaller and more uniform.

Reaction temperature also affects the size of the hybrid nanoparticles, and especially the size of the PDVB component. For batches synthesized at 45 and 65 °C, the average sizes change from Au 95 ± 2 nm/PDVB 200 nm ± 10 nm to nearly equal sizes Au 59 ± 2 nm/PDVB 60 ± 3 nm (Fig. 3a, b). This is because higher reaction temperatures result in faster polymer nucleation and larger numbers of nuclei, which makes the size of each particle smaller. A similar trend towards smaller Au NPs is observed, since the PDVB and Au NPs nucleate simultaneously, though their growth rates are different. However for even lower temperatures (25 °C) when the PDVB particles grow even more slowly, additional Au nucleations occur on their surface during growth stage, as evidenced by the differing Au NPs size (Fig. S2†). This consumes some of the $HAuCl_4$, creates several Au seeds per PDVB particle, and makes the overall Au NP sizes smaller. Fig. 3 shows the average sizes of Au-PDVB nanoparticles with typical images at different reaction temperatures in the optimal regime.

As seen in these experiments, the final morphology of the hybrid Au-PDVB nanoparticles is largely determined by the nucleation and growth of the Au and PDVB components. To monitor and understand the growth kinetics, we quenched the polymerization with large amounts of water at different stages of the reaction, and applied centrifugation to separate the intermediate products and observe their morphologies (Fig. 4a, b). Initially, nucleation of Au NPs occurs simultaneously with the polymerization of DVB *via in situ* redox reactions. Further growth of the PDVB follows a typical radical polymerization with a self-acceleration process as shown in Fig. 4b. It is difficult to distinctively observe initial stages of polymer layer formation due to its low electron density compared with the Au NPs. Beyond 2 h of reaction time, the size of the Au NPs increases nonlinearly from 54 to 127 nm and the size of PDVB from 11 to 246 nm (Fig. 4c). Although the size of the DVB droplets varies in the suspension, the growth of PDVB inside the DVB droplets is simultaneous and uniform. Therefore, we observe a steady and uniform increase of the size of the hybrid nanoparticles. The growth of the Au component was also independently monitored with UV-Vis spectra as shown in Fig. 4(c). There is no plasmon peak detected in the first 3 minutes of reaction, indicating there is no immediate nucleation of Au NPs even although there might be some intermediate reduction of $HAuCl_4$ to the Au^+ state. The absorption peak intensity and maximum gradually shifts (from 570 to 580 nm), matching the steady increase in the size of the Au NPs (Fig. 4d), indicating continuous exposure to the aqueous environment, until they eventually reach a plateau after 2 h. Noteworthy is that the growth of Au almost complete in the first 30 min (black curve, Fig. 4c). The small increase by 2 h may be due to Ostwald ripening from late-nucleated

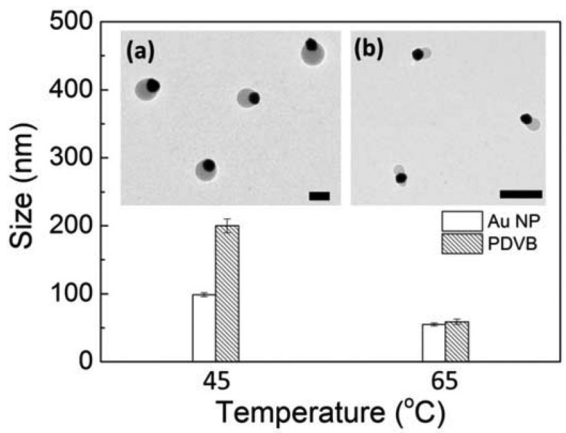

Fig. 3 Sizes of Au and PDVB components obtained at different temperatures. Insets are TEM images of asymmetric Au-PDVB hybrid nanoparticles synthesized at (a) 45 °C and (b) 65 °C. Scale bars are 200 nm.

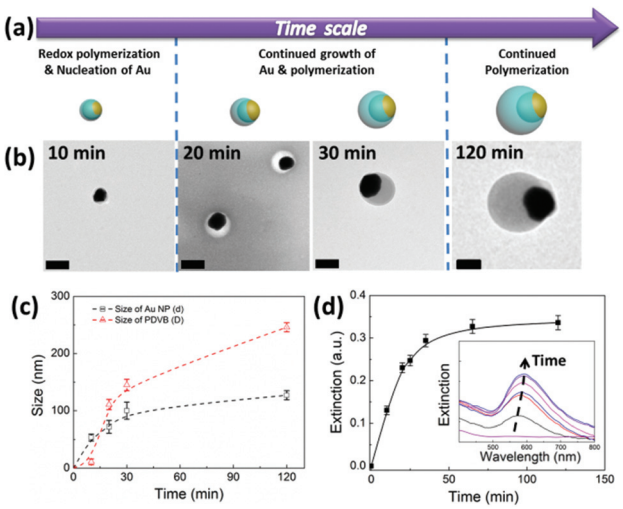

Fig. 4 Kinetics of growth of hybrid nanoparticles. (a) Scheme and (b) typical TEM images at different times, all scale bars are 100 nm. (c) Size changes of components of Au and PDVB with time. (d) Growth kinetics of Au component monitored with UV-Vis spectroscopy.

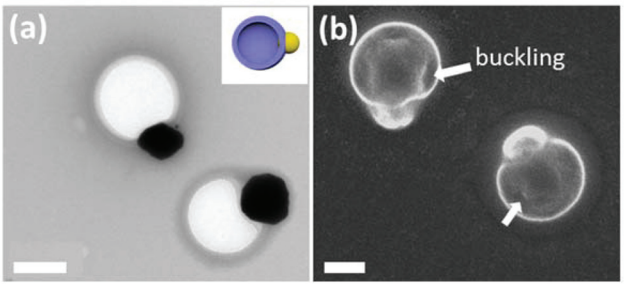

Fig. 5 (a) TEM and (b) SEM images of Au-PS Janus nanoparticles obtained using Styrene as the monomer. Inset is the scheme representing Au-PS hollow shell Janus hybrid nanoparticles. Scale bars are 200 nm.

particles which disappear into the larger ones. The growth of the PDVB follows characteristic dispersion polymerization kinetics.[22,23]

The growth rates of Au and PDVB thus are matched at initial stages due to the redox reaction between $HAuCl_4$ and DVB. Interfacial energy mismatches and competitive surface adsorption play a role in the relative kinetics before one reaches exhaustion of a reagent. In the later stages, when the $HAuCl_4$ is totally consumed, the growth of DVB continues only by radical polymerization. Some similar particles have been formed by other reaction mechanisms, *e.g.*, in the biphasic interfacial polymerization of Au and aniline.[14] The mechanism we resolve here, however, applies to other monomers as well, since if we use styrene as the monomer, we also observe the formation of Au-PS Janus nanoparticles as shown in Fig. 5. Here the PS is not crosslinked but can still form Janus particles which thus excludes the nonlinear swelling-induced anisotropic growth mechanism we have discovered previously.[12] Interestingly, rather than solid spheres, hollow PS capsules are formed (Fig. 5a), which further supports the idea that interfacial nucleation and polymerization is the key route to the formation of Janus hybrid nanoparticles. The polymerization efficiency of styrene droplets is lower than that of DVB, which is likely the main reason that only the surfaces of the droplets are polymerized. When dried from solution, the unreacted styrene in the interior evaporates, leaving a buckled shell behind (Fig. 5b).

Our method is likely to be applicable to a large number of monomers, including also conductive molecules. In a study with different environment and research focus similar Au/polypyrrole particles were apparently obtained by a room temperature reaction.[15,24] Though different temperatures were not investigated, the polydispersity observed for Ag on polypyrrole[24] and PS,[25] is similar to what we observe at 25 °C due to slow growth and multiple nucleation, so it is likely they were formed by the same mechanism. Having a detailed understanding of the reactions and kinetics involved, as depicted here, are important steps to further control and develop such energy- and material-efficient one-pot reactions. Further steps in developing the envisioned theranostic applications for these hybrid Janus particles will involve the incorporation of model drug molecules in the polymer components of the particles.[26,27]

4. Conclusions

This paper introduces a facile approach to synthesize asymmetric hybrid plasmonic nanoparticles made of Au and PDVB. The oxidative dispersion polymerization of DVB initiated by $HAuCl_4$ simultaneously creates both a highly cross-linked PDVB component and an adjacent Au NP. Here, PVP molecules act as a stabilizing agent for the polymerization, a stable interface for Au NPs nucleation and a competitive capping agent for the Au. They prevent coalescence of the particles and help generate the asymmetric growth. Because the DVB oligomers have to displace PVP from the Au surface, PDVB only partially wets the surface of Au NPs, thereby generating asymmetric growth of PDVB on the Au NPs. The size and monodispersity of the particles can be well controlled by the concentrations of $HAuCl_4$ and DVB, as well as by the reaction temperature. The growth kinetics of the hybrid nanoparticles were followed for Au-PDVB, as well as the Au-PS Janus nanoparticles, further elucidating their formation. Such one-pot formation opens up efficient, bio-inspired mechanisms for complex morphogenesis, which feature symmetry breaking, and independent reactions which maintain the lower symmetry.[28,29] The large polymer lobes create steric hindrance and the unique possibility of packing only 3 or 2 of the Au plasmonic cores touching each other. The ability for such selective aggregation has long been sought in SERS sensing and is a potential application for the hybrid Janus particles created by this and other methods. Further development of Janus nanoparticles with polymer and plasmonic components, as with the Au-PDVB shown here, is promising in several fields, including nano self-assembly, optics, sensing and medical applications.

Acknowledgements

The research was funded by ERC grants EMATTER 280078 and LINASS 320503, and EPSRC grants EP/G060649/1, and EP/L027151/1.

Notes and references

1 T. Ding, K. Song, K. Clays and C.-H. Tung, *Adv. Mater.*, 2009, **21**, 1936–1940.
2 T. Ding, Y. Tian, K. Liang, K. Clays, K. Song, G. Yang and C.-H. Tung, *Chem. Commun.*, 2011, **47**, 2429.
3 T. Ding, Y. Long, K. Zhong, K. Song, G. Yang and C.-H. Tung, *J. Mater. Chem. C*, 2014, **2**, 4100–4111.
4 T. Ding, K. Song, K. Clays and C.-H. Tung, *J. Nanosci. Nanotechnol.*, 2010, **10**, 7571–7573.

5 T. Ding, K. Song, K. Clays and C.-H. Tung, *Langmuir*, 2010, **26**, 11544–11549.
6 Z. W. Seh, S. Liu, S.-Y. Zhang, M. S. Bharathi, H. Ramanarayan, M. Low, K. W. Shah, Y.-W. Zhang and M.-Y. Han, *Angew. Chem., Int. Ed.*, 2011, **50**, 10140–10143.
7 M. Grzelczak and L. M. Liz-Marzan, *Langmuir*, 2013, **29**, 4652–4663.
8 S. C. Glotzer and M. J. Solomon, *Nat. Mater.*, 2007, **6**, 557–562.
9 X. Huang and M. A. El-Sayed, *Alexandria J. Med.*, 2011, **47**, 1–9.
10 T. Chen, M. X. Yang, X. J. Wang, L. H. Tan and H. Y. Chen, *J. Am. Chem. Soc.*, 2008, **130**, 11858–11859.
11 A. Ohnuma, E. C. Cho, P. H. C. Camargo, L. Au, B. Ohtani and Y. N. Xia, *J. Am. Chem. Soc.*, 2009, **131**, 1352–1353.
12 T. Ding, S. Smoukov and J. J. Baumberg, *J. Mater. Chem. C*, 2014, **2**, 8745–8749.
13 H. L. Xu, X. K. Liu, G. Su, B. Zhang and D. Y. Wang, *Langmuir*, 2012, **28**, 13060–13065.
14 H. Yabu, K. Koike, K. Motoyoshi, T. Higuchi and M. Shimomura, *Macromol. Rapid Commun.*, 2010, **31**, 1267–1271.
15 J. He, M. T. Perez, P. Zhang, Y. J. Liu, T. Babu, J. L. Gong and Z. H. Nie, *J. Am. Chem. Soc.*, 2012, **134**, 3639–3642.
16 S. Torza and S. G. Mason, *J. Colloid Interface Sci.*, 1970, **33**, 67–83.
17 S. X. Xing, Y. H. Feng, Y. Y. Tay, T. Chen, J. Xu, M. Pan, J. T. He, H. H. Hng, Q. Y. Yan and H. Y. Chen, *J. Am. Chem. Soc.*, 2010, **132**, 9537–9539.
18 L. Li, L. Y. Zhang, S. X. Xing, T. T. Wang, S. R. Luo, X. Q. Zhang, C. Liu, Z. M. Su and C. G. Wang, *Small*, 2013, **9**, 825–830.
19 K. K. Nanda, A. Maisels and F. E. Kruis, *J. Phys. Chem. C*, 2008, **112**, 13488–13491.
20 S. Badaire, C. Cottin-Bizonne, J. W. Woody, A. Yang and A. D. Stroock, *J. Am. Chem. Soc.*, 2007, **129**, 40–41.
21 J. J. Mock, D. R. Smith and S. Schultz, *Nano Lett.*, 2003, **3**, 485–491.
22 K. E. J. Barrett and H. R. Thomas, *J. Polym. Sci., Polym. Chem. Ed.*, 1969, **7**, 2621–2650.
23 S. F. Ahmed and G. W. Poehlein, *Ind. Eng. Chem. Res.*, 1997, **36**, 2597–2604.
24 S. Xing, L. H. Tan, T. Chen, Y. Yang and H. Chen, *Chem. Commun.*, 2009, 1653–1654.
25 C.-W. Wang, S.-J. Tseng, S.-F. Peng, Y.-K. Hwu and C.-K. Lin, *Nanotechnology*, 2012, **23**, 255103.
26 R. Bardhan, S. Lal, A. Joshi and N. J. Halas, *Acc. Chem. Res.*, 2011, **44**, 936–946.
27 Y. Xia, W. Li, C. M. Cobley, J. Chen, X. Xia, Q. Zhang, M. Yang, E. C. Cho and P. K. Brown, *Acc. Chem. Res.*, 2011, **44**, 914–924.
28 J. Graham, D. C. Freeman and J. Emlen, *Genetica*, 1993, **89**, 121–137.
29 A. R. Palmer, *Science*, 2004, **306**, 828–833.